J Inf Process Syst, Vol.18, No.5, pp.688~700, October 2022
https://doi.org/10.3745/JIPS.04.0256

ISSN 1976-913X (Print)
ISSN 2092-805X (Electronic)

JOURNAL OF INFORMATION PROCESSING SYSTEMS JIPS

# Designing a Magnetically Controlled Soft Gripper with Versatile Grasping Based on Magneto-Active Elastomer

Rui Li, Xinyan Li, Hao Wang, Xianlun Tang, Penghua Li, and Mengjie Shou*

**Abstract**

A composite bionic soft gripper integrated with electromagnets and magneto-active elastomers is designed by combining the structure of the human hand and the snake's behavior of enhancing friction by actively adjusting the scales. A silicon-based polymer containing magnetized hard magnetic particles is proposed as a soft finger, and it can be reversibly bent by adjusting the magnetic field. Experiments show that the length, width, and height of rectangular soft fingers and the volume ratio of neodymium–iron–boron have different effects on bending angle. The flexible fingers with 20 vol% are the most efficient, which can bend to 90° when the magnetic field is 22 mT. The flexible gripper with four fingers can pick up 10.51 g of objects at the magnetic field of 105 mT. In addition, this composite bionic soft gripper has excellent magnetron performance, and it can change surface like snakes and operate like human hands. This research may help develop soft devices for magnetic field control and try to provide new solutions for soft grasping.

**Keywords**

Biomimetics, Magnetic Actuation, Magnetic Particle-Filled Composite, Soft Gripper

## 1. Introduction

With the continuous development of technology, robots have been widely applied in various industries [1-4]. Traditional robots often have typical devices for holding, moving, and manipulating objects. However, these rigid devices are usually restricted in narrow fields. For example, the transportation of objects with smooth surfaces, fresh food, and fragile and deformable objects need to ensure that objects are not damaged while not leaving a mark. For these fields, traditional rigid devices are difficult to meet the requirements. Therefore, a device that can be changed according to the grasped object without leaving a mark is an urgent problem to be solved.

Soft grabbing has become a hot research direction. Generally, soft grippers can be divided into three categories: actuation type, stiffness adjustment type, and surface adhesion capacity adjustment type. Although these soft grippers have their own advantages, some shortcomings still remain. For example, the electroactive polymer clamps have a fast response speed [5], but they generally require more than a kilovolt voltage to generate sufficient stress. Soft grippers based on memory alloy can be controlled remotely [6], but they need a long time to adjust the temperature.



Manuscript received January 27, 2021; first revision March 25, 2021; accepted April 26, 2021.

* **Corresponding Author:** Mengjie Shou (shoumj@cqupt.edu.cn)
School of Automation, Chongqing University of Posts and Telecommunications, Chongqing, China (lirui@cqupt.edu.cn, lixinyan2029@163.com, 595612931@qq.com, tangxl@cqupt.edu.cn, liph@cqupt.edu.cn, shoumj@cqupt.edu.cn)

From the above discussion, smart materials are often used to make soft grippers. Among the intelligent materials, the magneto-active elastomer (MAE) is an ideal intelligent optional material for making soft grippers because of its fast response, magnetic actuation, and magnetically controlled variable stiffness damping. However, these fixtures can only grasp extremely light objects. The main reason is that traditional MAE is filled with low residual magnetic particles, such as carbonyl iron powder [7]. Thus, by replacing traditional low remanence filled particles with high magnetization saturation strength, flexible MAEs have a large deformation under the changing external magnetic fields [8]. Moreover, its performance can be further improved when the MAEs are fabricated in an external magnetic field [9,10]. When the MAE is made into a thin film, the magnetic particles will be magnetized, which can produce strong deformation ability under a small magnetic field [11]. Therefore, the optimized MAE is an ideal multifunctional actuator in complex environments [12,13].

However, the magnetic field of the current magnetic control fixtures is distributed outside of the structure; hence, the objects inside the magnetic field should be ensured not to be interfered by the external magnetic field, thereby limiting its application. More importantly, the magnetic field also affects the friction performance [14], which has not been considered in the current magnetic control fixture. Therefore, improving the grasping behavior by changing the surface friction performance is an important research direction.

To widen the application scenes of bionic soft grab and investigate the influence of magnetic field on friction performance, a composite bionic soft grab structure that integrates electromagnet and MAE was proposed by imitating the structure of hand and snake's behavior of adjusting scales. To optimize grip performance, the effect of the size ratio of the electromagnet on the magnetic field and the size of the soft finger on the bending angle were studied by simulation. The experiments verified that the soft gripper could be used to grasp different objects. This composite bionic soft gripper could provide a new approach and some inspiration for the integrated optimization of soft gripping.

# 2. Structure

## 2.1 Conceptual Design

On the basis of the industrial demand for soft grips, a composite bionic soft gripper is designed, as shown in Fig. 1. The soft gripper mainly includes two parts: electromagnet and soft fingers. As a control mechanism, electromagnet plays the role of supporting and transmitting control signals, similar to a palm. The soft fingers not only imitate the structure of human fingers but also imitate the snake’s behavior of adjusting scales [15]. Under the control of the magnetic field, all flexible fingers bend toward the center of an electromagnet and increase the surface roughness.

## 2.2 Electromagnet Design

Generally, the electromagnet uses a closed structure to make the air gap in the magnetic circuit as small as possible to produce a larger magnetic field there. However, the closed structure is not conducive to grasping. Thus, in the soft gripper, one end of the electromagnet is designed to be unclosed, and the magnetic field is transmitted to the soft finger through the air, as shown in Fig. 2(a).

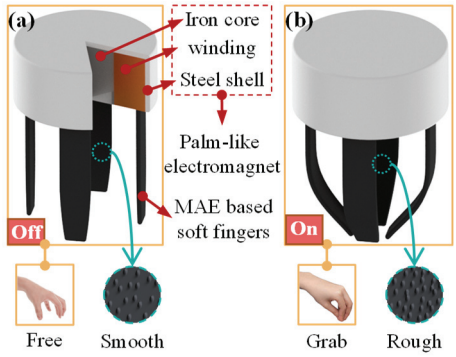


**Fig. 1.** Schematic of a composite bionic flexible gripper in (a) nonworking state with a smooth surface and (b) working state with a rough surface.

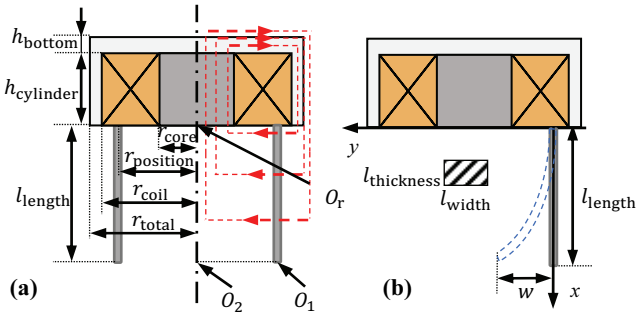


**Fig. 2.** The 2D models of the soft gripper: (a) magnetic circuit model and (b) bending model.

However, this design also makes the magnetic field decay rapidly in the air. Thus, the parameter optimization of the electromagnet is extremely important. Hence, the magnetic field simulation must be performed to optimize the dimensions of the electromagnet to meet the minimum driving magnetic field of the soft finger. Before the simulation, the magnetic field of some important points in the structure must be estimated. In Fig. 2(a), $h_{\text{cylinder}}$ and $r_{\text{core}}$ are the height and radius of the iron core, respectively; $h_{\text{bottom}}$ is the thickness of the upper disk-shaped steel shell; $r_{\text{coil}}$ is the outer diameter of the coil; $r_{\text{position}}$ is the distance between the center point of the fixed end of the soft finger and the axis of the electromagnet; $r_{\text{total}}$ is the radius of the entire electromagnet; $l_{\text{length}}$ is the length from the fixed end to the free end of the soft finger; $O_{\text{r}}$ is the center point of the surface of the iron core; $O_1$ is the center point of the upper surface of the free end of the finger; and $O_2$ is the point on the axis of the electromagnet and is 2 m away from the bottom of the electromagnet. The magnetic flux densities generated by the electromagnets at three points $O_r$, $O_1$, and $O_2$ are $B_r$, $B_1$, and $B_2$, respectively.

According to Biot–Savart's law, $B_r$ can be expressed as

$$B_r = \frac{\mu_{iron} IN}{2}\left(\sqrt{2} + \frac{h_{cylinder}}{\sqrt{h_{cylinder}^2 + r_{coil}^2}} - \frac{h_{cylinder}}{\sqrt{h_{cylinder}^2 + r_{core}^2}}\right), \tag{1}$$

where $\mu_{\text{iron}}$ is the magnetic permeability of iron, $I$ represents the current in the electromagnet, and $N$ is the number of turns of the coil. $B_2$ can be expressed as follows [16]:

$$B_2 = \frac{B_r}{2}\left(\frac{h_{cylinder} + l_{length}}{\sqrt{\left(h_{cylinder} + l_{length}\right)^2 + r_{coil}}} - \frac{h_{cylinder}}{\sqrt{h_{cylinder}^2 + r_{coil}}}\right). \tag{2}$$

To simplify the model, the magnetic flux on the plane parallel to the surface of the electromagnet and that perpendicular to the axis of the electromagnet is considered the same; thus, $B_1 \approx B_2$. This simplified model can be used to calculate the magnetic field produced by the electromagnet, and the simulation of the magnetic circuit can be preliminarily assisted.

## 2.3 Modeling the MAE Deformation and Surface Roughness

The characteristics of MAE change under influence of the magnetic field. As shown in Fig. 2(b), bending deformation is one of the phenomena, and it is also the most important behavior in grasping. The force bending soft fingers comes from the interaction between the hard magnetic particles and the electrified coil. The magnetic particles in the MAE can be considered as dipoles. The magnetization of magnetic particles can be obtained using the Fröhlich–Kennely formula, as shown as follows:

$$M = \frac{M_S H(\mu_r - 1)}{(\mu_r - 1)H + M_S}, \tag{3}$$

where

$$H = \frac{B_r}{\mu_0}, \tag{4}$$

where $M_s$ and $\mu_r$ represent the magnetic saturation and relative permeability of the neodymium–iron–boron (NdFeB) particles, respectively. The variation of the shear modulus of the MAE can be calculated by the dipole model, as shown as follows:

$$\Delta G = 4.808\mu_0\varphi M^2\left(\frac{R}{d}\right)^3, \tag{5}$$

where $R$, $\varphi$, and $d$ are the average radius, volume fraction, and distance of particles, respectively. Then, the variation of Young's modulus can be expressed as

$$\Delta E = 2\Delta G(1 + \nu) \approx 3\Delta G, \tag{6}$$

where $\nu$ is the Poisson's ratio of the MAE. The equivalent magnetic force applied to a unit area of the MAE can be expressed as

$$F_{\mathrm{m}} = \frac{\mu_0\mu_{\mathrm{m}}(\mu_{\mathrm{m}} - 1)}{2}\left\{\left[H_{0\mathrm{z}}^{+}\left(\frac{l_{\mathrm{thickness}}}{2}\right)^2\right] - \left[H_{0\mathrm{z}}^{+}\left(-\frac{l_{\mathrm{thickness}}}{2}\right)^2\right]\right\}, \tag{7}$$

where

$$\mu_{\mathrm{m}} = 1 + \frac{3\varphi(4 + \varphi)}{4(1 - \varphi)}, \tag{8}$$

where $\mu_{\mathrm{m}}$ is the relative permeability of the MAE; and $H_{0\mathrm{z}}^{+}\left(\frac{l_{\mathrm{thickness}}}{2}\right)$ and $H_{0\mathrm{z}}^{+}\left(-\frac{l_{\mathrm{thickness}}}{2}\right)$ are the normal components of the magnetic field intensity on the upper and lower surfaces, respectively. The deformation of the MAE can be obtained by Euler–Bernoulli beam theory as follows:

$$w = \frac{F_{\mathrm{m}} l_{\mathrm{width}} l_{\mathrm{length}}^4}{8EI}, \tag{9}$$

where $E$ is the Young's modulus of the MAE under the magnetic field, and $I$ is the moment of inertia of the beam. Thus, the bending displacement of soft fingers can be calculated by using an iterative algorithm based on Eq. (9). When the direction of the applied magnetic field is the same as the direction of the magnetic dipole moment, the interaction force between the magnetized NdFeB particles can be expressed as follows:

$$F_{ij} = -\frac{3\mu_0[3(m_i \cdot r_0)(m_j \cdot r_0) - m_i m_j]}{4\pi d^4}, \tag{10}$$

where $m_i$ and $m_j$ are the magnetic dipole moment of and particles $i$ and $j$ in the magnetic field, respectively; and $r_0$ is the direction vector of the magnetic moment. Assuming that all magnetic dipole moments are equal, Eq. (10) can be reduced to

$$F_{ij} = -\frac{3\mu_0 m^2}{4\pi d^4}(1 - 3\cos^2\theta), \tag{11}$$

where $\theta$ is the angle between the line connecting the central point of the $i$th and $j$th magnetic dipole and the direction of the applied magnetic field. The magnetically induced stress generated by the NdFeB particles under the interaction of the magnetic force $F_{ij}$ can be expressed as

$$\sigma_{ij} = E \cdot \varepsilon, \tag{12}$$

where $\varepsilon$ is the small strain of the MAE. The small deformation of the MAE is caused by these magnetically induced stresses.

# 3. Prototype and Experimental Setup

## 3.1 Magnetic Field Simulation

The magnetic field produced by the electromagnet determines the magnetic force of flexible fingers, and the magnetic force can indirectly affect the grasping force. Therefore, to optimize the grasping ability, Multiphysics software (COMSOL Inc., Palo Alto, CA, USA) must be used to design and optimize the dimensional parameters of the electromagnet to make the magnetic field as large as possible.

Given that the magnetic field produced by the electromagnet is proportional to its size, $r_{\text{total}}$ and $h_{\text{cylinder}} + h_{\text{bottom}}$ are set as the fixed value in the simulation. Then, the influence of the proportion of iron core, coil, and magnetic conducting shell in the electromagnet on the magnetic field is evaluated. At the same time, $r_{\text{position}}$ also affects the magnitude of the magnetic field. Thus, the average value of the magnetic flux on the four-line segments is used as an evaluation index during the simulation to evaluate the magnitude of the magnetic field of different size parameters without considering $r_{\text{position}}$. The four line segments take the central axis of the electromagnet as the vertical line and have a length equal to $2r_{\text{total}}$ [16]. The distances between them and the uncovered surface of the electromagnet are $\frac{l_{\text{length}}}{4}$, $\frac{l_{\text{length}}}{2}$, $\frac{3l_{\text{length}}}{4}$, and $l_{\text{length}}$. If the length of soft fingers is extremely long, then the magnetic field cannot effectively reach the free end of the soft fingers; thus, the maximum length of the soft fingers must be limited. To ensure that the fingers will not overlap when the bending angle reaches 45°, the maximum value of the length $l_{\text{length}}$ of the soft fingers is limited to $\sqrt{2}r_{\text{total}}$. On the basis of the above conditions,

the simulation results are shown in Fig. 3.

In Fig. 3, $r_{\mathrm{coil}} - r_{\mathrm{core}}$ is half of the difference between the outer and inner diameters of the coil, $k_{\mathrm{h}} = h_{\mathrm{cylinder}}/(h_{\mathrm{cylinder}} + h_{\mathrm{bottom}})$, $k_{\mathrm{r1}} = r_{\mathrm{core}}:(r_{\mathrm{coil}} - r_{\mathrm{core}})$, and $k_{\mathrm{r2}} = r_{\mathrm{coil}}/r_{\mathrm{total}}$. The values of $k_{\mathrm{h}}$ and $k_{\mathrm{r1}}$ cannot be equal to 0 and 1 due to the physical relationship. When $k_{\mathrm{h}}$ is 0.025 and 0.975, the height of the core and coil is minimum and maximum, respectively; and the same is true for $k_{\mathrm{r2}}$. As shown in Fig. 3, the magnetic field increases with $k_{\mathrm{h}}$. For each $k_{\mathrm{h}}$, the magnetic field increases with $k_{\mathrm{r2}}$. Thus, the magnetic field increases with the volume ratio of the core and the coil. Moreover, for any $k_{\mathrm{h}}$, when $k_{\mathrm{r1}} > 1$, the magnetic field decreases with the increase of $k_{\mathrm{r1}}$. When $k_{\mathrm{r1}} < 1$, there exist two cases based on the value of $k_{\mathrm{h}}$. One is that when $k_{\mathrm{h}} < 0.1$, the magnetic field decreases slightly as $k_{\mathrm{r1}}$ increases. The other is that when $k_{\mathrm{h}} \geq 0.1$, the magnetic field increases with $k_{\mathrm{r1}}$. In addition, the growth rate of the magnetic field increases with $k_{\mathrm{h}}$. Moreover, when the value of $k_{\mathrm{r1}}$ ranges from 1:5 to 1:1, the magnetic field has a maximum value. In other words, when the size of the core and the coil occupy a relatively large portion of the electromagnet, half of the difference between the inner and outer diameters of the coil is slightly larger than the radius of the core to generate a larger magnetic field.

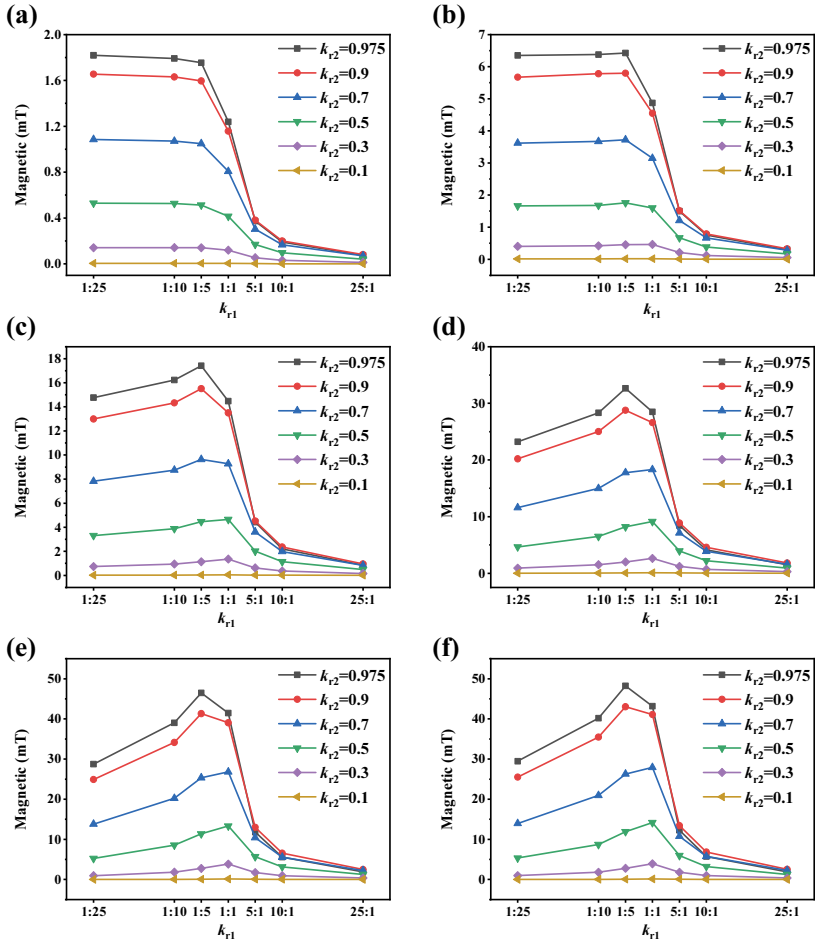


**Fig. 3.** Mean value of the magnetic field generated by different-sized electromagnets on four-line segments: (a) $k_{\mathrm{h}} = 0.025$, (b) $k_{\mathrm{h}} = 0.1$, (c) $k_{\mathrm{h}} = 0.3$, (d) $k_{\mathrm{h}} = 0.3$, (e) $k_{\mathrm{h}} = 0.6$, and (f) $k_{\mathrm{h}} = 0.975$.

## 3.2 Finger Simulation

In addition to electromagnets, soft fingers also need to be studied. The bending range of soft fingers affects the shape and size of the items it can grasp. The larger bending range can make flexible grippers cope with the more diversified objects, which means improving the adaptability of the gripper. According to the Euler–Bernoulli beam theory [17], the size of the soft fingers will affect the bending range. Therefore, the size of the soft fingers must be simulated, and the influence of their length, width, and height on bending should be investigated. The effect of the position $r_{\text{position}}$ of soft fingers on the electromagnet on the bending angle is also studied in this paper.

Given that the structure of the gripper is symmetrical, only one finger is modeled and simulated in Multiphysics software. The control variable method is used in the simulation. Under the same magnetic field, one of $l_{\text{length}}$, $l_{\text{width}}$, $l_{\text{thickness}}$, and $r_{\text{position}}$ is changed, and the remaining three is fixed to study their effects on the bending range. The angle between the connection between the fixed and unfixed ends of the soft finger and the original position is used as the evaluation index.

Fig. 4 shows the effects of different parameters on the bending angle, and each parameter is normalized by dispersion within its variation range. The range of each parameter is $0 \le l_{\text{length}} \le \sqrt{2}r_{\text{total}}$, $0 \le l_{\text{width}} \le 2r_{\text{total}}$, $0 \le l_{\text{thickness}} \le r_{\text{total}}$, and $r_{\text{core}} \le r_{\text{position}} \le r_{\text{total}}$. Fig. 4 shows that $l_{\text{length}}$ and $l_{\text{thickness}}$ have greater effects on bending deformation, whereas $l_{\text{width}}$ and $r_{\text{position}}$ have smaller effects on it. As $l_{\text{length}}$ and $r_{\text{position}}$ increase, the bending angle also gradually increases. When $l_{\text{length}}$ and $r_{\text{position}}$ grow to a certain size, the bending angle no longer increases, whereas the opposite is true for $l_{\text{thickness}}$. The bending angle decreases slightly with the increase of $l_{\text{width}}$. Combined with the simulation results, the size of the soft fingers can be selected according to the characteristics of objects. Moreover, the influence of the magnetic field direction on the bending deformation fingers is investigated.

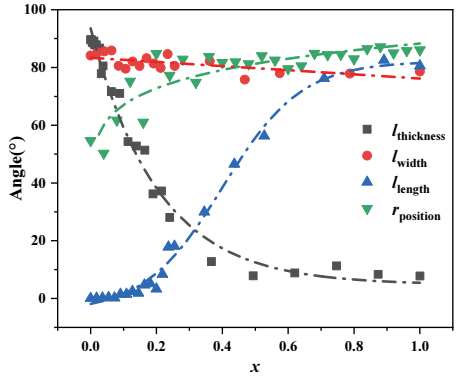


**Fig. 4.** Effects of normalized $r_{\text{position}}$, $l_{\text{length}}$, $l_{\text{width}}$, and $l_{\text{thickness}}$ on the bending angle of soft fingers.

In Fig. 5, the magnetization direction of soft fingers is along the negative direction of the y-axis, the arrow indicates the magnitude and direction of the magnetic flux, and the color indicates stress. When the direction of the magnetic field changes, the bending direction of the soft fingers also changes. Thus, even if the free end of flexible grippers is smaller than the dimension of objects, it can adjust the direction of the magnetic field to make the flexible fingers open and then close, which can further enhance the gripping adaptability of flexible grippers.

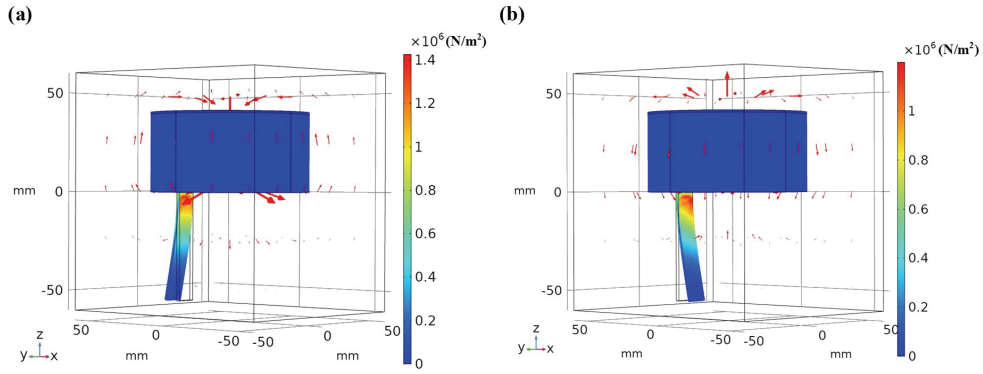


**Fig. 5.** Schematic of the stress distribution of a soft gripper under (a) positive and (b) negative magnetic fields.

## 3.3 Prototype Construction

On the basis of the simulation results in Sections 3.1 and 3.2, a set of dimensional parameters with better results are selected to verify the performance of the soft grippers. The prototype device is a preliminary experiment. It is verified without a magnetically permeable shell but with a coil core and soft fingers. Table 1 shows the main structural dimensions in Figs. 2 and 3. The size of other parts used for assembly is determined by the assembly relationship. On this basis, a prototype of a soft gripper with magnetic field control is manufactured and assembled. The installation of the soft gripper is completed by fixing one end of the soft fingers to the uncovered end of the electromagnet. This prototype has a height of about 90 mm and a diameter of about 80 mm.

**Table 1.** Main dimensions of the prototype soft gripper

| Sub-unit | Symbol | Dimension (mm) |
|---|---|---|
| Electromagnet | $r_{\text{core}}$ | 11 |
| | $r_{\text{coil}}$ | 40 |
| | $h_{\text{cylinder}}$ | 40 |
| Soft finger | $l_{\text{length}}$ | 50 |
| | $l_{\text{thickness}}$ | 2 |
| | $l_{\text{width}}$ | 10 |
| | $r_{\text{position}}$ | 31 |
| | $n$ | 4 |

## 3.4 Experimental Setup

Factors that affect the bending angle of soft fingers are not only the size but also the content of hard magnetic particles. Therefore, soft fingers with different volume fractions of hard magnetic particles should be prepared to study their influence on the bending angle. The soft fingers containing different volume fractions (5, 10, and 20 vol%) of NdFeB are prepared according to the method of Fig. 6(a). Then, the device shown in Fig. 6(b) is used to measure the relationship between its magnetic field and deformation. One end of the soft finger is fixed on a connecting member, and the connecting member is connected to a lead screw (direction of a plumb) coaxial with the motor. The soft finger is driven by the

motor controlled by the host computer and moves vertically toward the NdFeB magnet at a certain speed. Every time a certain distance is moved, the position of the free end of the soft finger relative to the fixed end and the magnetic flux density experienced by the free end are measured. The experiment also includes the use of the mechanical properties of the testing machine to test the stress–strain relationship of samples, as well as the demonstration of a soft gripper to grab objects. Finally, the surface roughness of the samples under different magnetic fields is also tested. Five points are taken on each sample, and each point is tested 10 times, and the average of all data is taken as the roughness of the sample.

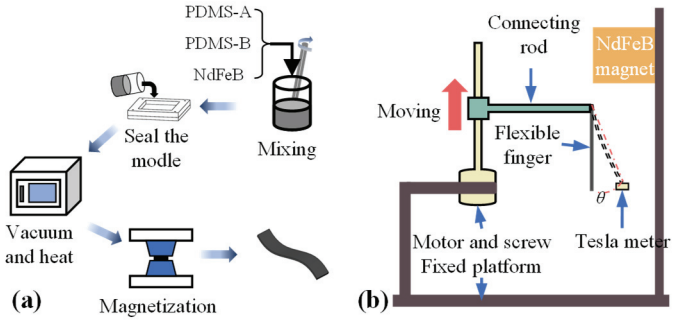


**Fig. 6.** Schematic of (a) soft finger preparation and (b) bending angle testing device.

# 4. Performance Analysis

## 4.1 Results and Discussion

This section shows various test results for a soft finger. Fig. 7(a) shows the relationship between the bending angle and magnetic flux of a soft finger with different volume fractions of NdFeB. As shown in Fig. 7(a), the magnetic field driving the soft finger to bend to 90° decreases with the increase in the volume ratio of NdFeB in the soft finger. The 5 vol% soft finger requires a magnetic field of at least 46.4 mT to drive the soft finger to 90°; the 10 vol% soft finger requires 39.9 mT, and the 20 vol% soft finger requires only 22 mT. The smaller the magnetic field required to drive to 90° is, the greater the bending angle under the same external magnetic field will be, the easier it will be for soft grippers to deal with different objects, and the more energy-efficient it will be. In addition, the bending repeatability of the soft finger is excellent, and the original state can be restored after the magnetic field is removed.

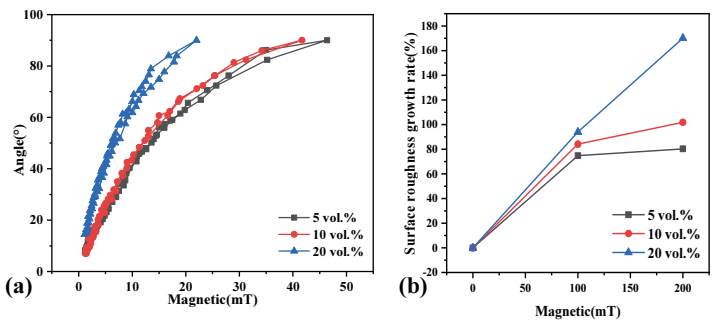


**Fig. 7.** Relationship between the magnetic flux and (a) bending angle and (b) surface roughness.

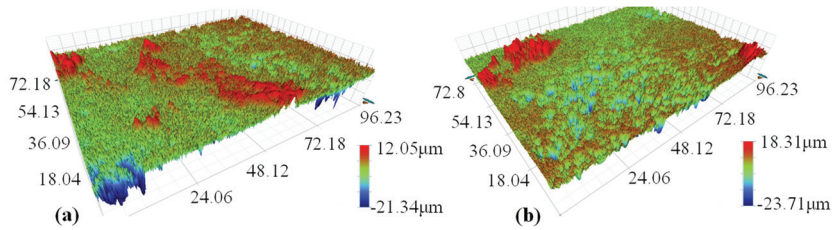


**Fig. 8.** White light interferometer test results of a typical MAE with 20 vol%: (a) without a magnetic field and (b) with magnetic field (200 mT).

Fig. 7(b) shows that the surface roughness of the soft finger increases with the magnetic field. The growth rate of surface roughness increases with the volume ratio of NdFeB. Thus, a soft finger can act like a snake, using magnetic fields to enhance surface friction. The comparison of Fig. 8(a) and 8(b) shows that the surface of the soft finger after applying the magnetic field has more convex peaks. Thus, the surface becomes rough, which can increase friction when gripping the item.

## 4.2 Grab Demo

This section shows the process of grabbing items with an integrated magnetron soft gripper. First, the object is placed directly under the flexible gripper. As the electromagnet is energized, all the flexible fingers bend toward the center. Then, the soft gripper is artificially lifted, and it picks up the object.

Fig. 9 briefly illustrates the process of grabbing two items by a magnetron soft gripper. Each row represents an entire process (initial, gripping, and lifting) of attempting to manipulate an object from bottom to top. The white dotted line is the sign of the bending direction of soft fingers, and the orange dotted line is the sign of the object to be grabbed. The object in Fig. 9(a) is a cylindrical hard rubber with a diameter of 28 mm, a height of 9 mm, and a weight of 10.51 g. The maximum value of a magnetic field on the surface of the electromagnet is 105 mT. The weight of an object that can be grasped per 1 mT is represented as the grasping ability value of a soft gripper controlled by a magnetic field. The gripping capacity value of this bionic soft gripper with four fingers is about 0.1 g/mT, and the value of the magnetron clamp using an external magnetic field method in [18] is 0.051 g/mT. This enhancement is due to the integrated structure of composite bionics. The integrated structure of coil and magnetic sensitive rubber designed by imitating human hand makes the flexible gripper more efficient. Imitating the behavior of snakes to adjust surface roughness also enhances the grasping ability of the soft gripper. Fig. 9(b) shows the process of grasping the cylindrical foam. The cylindrical foam has not been damaged in the process of grasping; thus, grasping objects with the soft gripper is safe. This integrated magnetically controlled soft gripper has broad application prospects in industrial production and other fields.

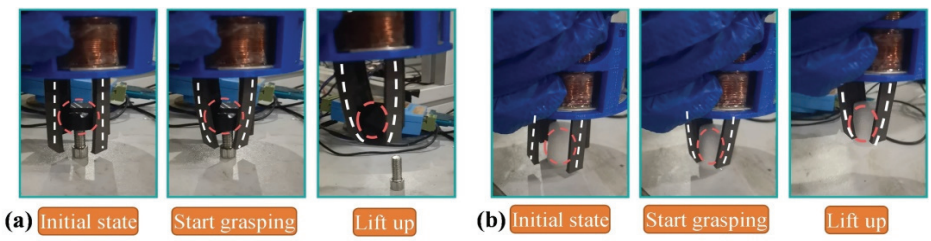


**Fig. 9.** Demonstration of grasping objects with soft gripper: (a) hard rubber with a smooth surface and (b) softer foam.

## 5. Conclusion

In this work, an integrated soft gripper structure with an electromagnet and a soft finger is proposed, which imitates the structure of human hands and the behavior of snakes adjusting the surface. The effect of the ratio between the electromagnet components on the magnetic flux generated by the electromagnet is simulated. When the ratio of the core radius to the coil wall thickness is between 1:5 and 1:1, the electromagnet can generate the largest magnetic field. Moreover, the magnetic bending angle of the soft finger is highly sensitive to the length and thickness of the soft finger and the volume fraction of the hard magnetic particles, and it is not sensitive to the thickness and position of the soft finger. The flexible fingers with 20 vol% are bent to 90° at the magnetic field of 22 mT. The experiment also proves that the soft finger increases the surface roughness under the action of magnetic fields, which indirectly enhances the grasping behavior. Finally, the soft gripper without a steel shell can grab different objects. Its grasping capacity is at least 0.1 g/mT. On the basis of the characteristics demonstrated in this work, the integrated magnetron soft gripper improves the performance and provides new methods for magnetron device integration. The magnetron soft gripper also has broad application prospects in many fields.

## Acknowledgement

We acknowledge the financial support for this work provided by the National Natural Science Foundation of China (52075063, 52105088, and 52211540394), the Innovation Research Group of Universities in Chongqing (CXQT20016), the Special Key Project of Technological Innovation and Application Development in Chongqing (cstc2019jscx-fxydX0085), the High-Level Foreign Expert Introduction Program (G2022035005L), and the Cooperation Project Between Undergraduate Universities in Chongqing and Institutions Affiliated with the Chinese Academy of Sciences (HZ2021018). The authors would like to take this opportunity to express their gratitude to the sponsors.

## References

[1] P. M. Chu, S. Cho, J. Park, S. Fong, and K. Cho, "Enhanced ground segmentation method for Lidar point clouds in human-centric autonomous robot systems," *Human-centric Computing and Information Sciences*, vol. 9, article no. 17, 2019. https://doi.org/10.1186/s13673-019-0178-5

[2] J. Kunhoth, A. Karkar, S. Al-Maadeed, and A. Al-Ali, "Indoor positioning and wayfinding systems: a survey," *Human-centric Computing and Information Sciences*, vol. 10, article no. 18, 2020. https://doi.org/10.1186/s13673-020-00222-0

[3] M. W. Akhtar, S. A. Hassan, R. Ghaffar, H. Jung, S. Garg, and M. S. Hossain, "The shift to 6G communications: vision and requirements," *Human-centric Computing and Information Sciences*, vol. 10, article no. 53, 2020. https://doi.org/10.1186/s13673-020-00258-2

[4] Y. Byun, S. Oh, and M. Choi, "ICT agriculture support system for chili pepper harvesting," *Journal of Information Processing Systems*, vol. 16, no, 3, pp. 629-638, 2020.

[5] J. Shintake, S. Rosset, B. Schubert, D. Floreano, and H. Shea, "Versatile soft grippers with intrinsic electroadhesion based on multifunctional polymer actuators," *Advanced Materials*, vol. 28, no. 2, pp. 231-238, 2016.

[6] A. Villanueva, C. Smith, and S. Priya, "A biomimetic robotic jellyfish (Robojelly) actuated by shape memory alloy composite actuators," *Bioinspiration & Biomimetics*, vol. 6, no. 3, article no. 036004, 2011. https://doi.org/10.1088/1748-3182/6/3/036004

[7] R. Li, M. Zhou, M. Wang, L. Liu, and P. A. Yang, "Self-sensing characteristics of vibration isolation bearing based on modified magneto-rheological elastomer," *Modern Physics Letters B*, vol. 32, no. 34-36, article no. 1840082, 2018. https://doi.org/10.1142/S0217984918400821

[8] G. Z. Lum, Z. Ye, X. Dong, H. Marvi, O. Erin, W. Hu, and M. Sitti, "Shape-programmable magnetic soft matter," *Proceedings of the National Academy of Sciences of the United States of America*, vol. 113, no. 41, pp. E6007-E6015, 2016.

[9] S. Marchi, A. Casu, F. Bertora, A. Athanassiou, and D. Fragouli, "Highly magneto-responsive elastomeric films created by a two-step fabrication process," *ACS Applied Materials & Interfaces*, vol. 7, no. 34, pp. 19112-19118, 2015.

[10] S. R. Mishra, M. D. Dickey, O. D. Velev, and J. B. Tracy, "Selective and directional actuation of elastomer films using chained magnetic nanoparticles," *Nanoscale*, vol. 8, no. 3, pp. 1309-1313, 2016.

[11] W. Hu, G. Z. Lum, M. Mastrangeli, and M. Sitti, "Small-scale soft-bodied robot with multimodal locomotion," *Nature*, vol. 554, no. 7690, pp. 81-85, 2018.

[12] Y. Kim, H. Yuk, R. Zhao, S. A. Chester, and X. Zhao, "Printing ferromagnetic domains for untethered fast-transforming soft materials," *Nature*, vol. 558, no. 7709, pp. 274-279, 2018.

[13] V. Q. Nguyen, A. S. Ahmed, and R. V. Ramanujan, "Morphing soft magnetic composites," *Advanced Materials*, vol. 24, no. 30, pp. 4041-4054, 2012.

[14] R. Li, D. Ren, X. Wang, X. Chen, S. Chen, and X. Wu, "Tunable friction performance of magneto-rheological elastomer induced by external magnetic field," *Journal of Intelligent Material Systems and Structures*, vol. 29, no. 2, pp. 160-170, 2018.

[15] H. Marvi and D. L. Hu, "Friction enhancement in concertina locomotion of snakes," *Journal of the Royal Society Interface*, vol. 9, no. 76, pp. 3067-3080, 2012.

[16] G. P. Hatch and R. E. Stelter, "Magnetic design considerations for devices and particles used for biological high-gradient magnetic separation (HGMS) systems," *Journal of Magnetism and Magnetic Materials*, vol. 225, no. 1-2, pp. 262-276, 2001.

[17] J. M. Gere and S. P. Timoshenko, *Deflections of Beams*. Heidelberg, Germany: Springer, 1991.

[18] S. Qi, H. Guo, J. Fu, Y. Xie, M. Zhu, and M. Yu, "3D printed shape-programmable magneto-active soft matter for biomimetic applications," *Composites Science and Technology*, vol. 188, article no. 107973, 2020. https://doi.org/10.1016/j.compscitech.2019.107973

**Rui Li** **https://orcid.org/0000-0003-1061-2951**

He received his B.S. degree in 1999 from Chongqing University of Technology, and received his M.S. degree and Ph.D. degree from Chongqing University, in 2004 and 2009, respectively. His current position is a professor in Chongqing University of Posts and Telecommunications. His main research interests include intelligent detection technology, friction control, and intelligent mechanical structure system.

**Xinyan Li** **https://orcid.org/0000-0003-4193-8807**

She received a B.S. degree in Electronic Information Engineering at Chengdu University and obtained a M.S. degree in Engineering in Control Science and Engineering at Chongqing University of Posts and Telecommunications. Her research interests are flexible intelligent sensing and multifunctional nanomaterials.

**Hao Wang** **https://orcid.org/0000-0001-7041-4987**

He received a B.S. degree in Electrical Engineering and Automation form Jianghan University and obtained a M.S. degree at Chongqing University of Posts and Telecommunications. His research interests are magneto-rheological materials.

**Xianlun Tang** **https://orcid.org/0000-0002-9174-7366**

He received his M.S. and Ph.D. degrees from Chongqing University in 2002 and 2007, respectively. He is currently a professor at Chongqing University of Posts and Telecommunications. His research interests cover pattern recognition and artificial intelligent, human-computer interaction system, service robot control.

**Penghua Li** **https://orcid.org/0000-0003-0615-7781**

He received the B.S. degree in Electronic Engineering and the Ph.D. degree in Control Theory and Control Engineering from University of Chongqing in 2008 and 2012, respectively. He is currently a Professor at Chongqing University of Posts and Telecommunications. His research fields include neural network theory and its application in time series processing, image recognition, battery health state monitoring.

**Mengjie Shou** **https://orcid.org/0000-0002-4369-1177**

He received the B.S. and Ph.D. degree from Chongqing University in 2015 and 2020, respectively. He is currently a lecturer affiliated with School of Automation, Chongqing University of Posts and Telecommunications. His main research interests focus on intelligent material, structure and system.